ELSEVIER

Journal of Biomechanics ▮ (▮▮▮▮) ▮▮▮–▮▮▮

JOURNAL OF BIOMECHANICS

www.elsevier.com/locate/jbiomech
www.JBiomech.com

Reduction of neuromuscular redundancy for postural force generation using an intrinsic stability criterion

Nathan E. Bunderson[a], Thomas J. Burkholder[b], Lena H. Ting[a,b,*]

[a]*The Wallace H. Coulter Department of Biomedical Engineering at Georgia Tech and Emory University, 313 Ferst Drive, Atlanta, GA 30322-0535, USA*
[b]*School of Applied Physiology, Georgia Institute of Technology, Atlanta, GA, USA*

Accepted 6 February 2008

Abstract

Postural control requires the coordination of multiple muscles to achieve both endpoint force production and postural stability. Multiple muscle activation patterns can produce the required force for standing, but the mechanical stability associated with any given pattern may vary, and has implications for the degree of delayed neural feedback necessary for postural stability. We hypothesized that muscular redundancy is reduced when muscle activation patterns are chosen with respect to intrinsic musculoskeletal stability as well as endpoint force production. We used a three-dimensional musculoskeletal model of the cat hindlimb with 31 muscles to determine the possible contributions of intrinsic muscle properties to limb stability during isometric force generation. Using dynamic stability analysis we demonstrate that within the large set of activation patterns that satisfy the force requirement for posture, only a reduced subset produce a mechanically stable limb configuration. Greater stability in the frontal-plane suggests that neural control mechanisms are more highly active for sagittal-plane and for ankle joint control. Even when the limb was unstable, the time-constants of instability were sufficiently great to allow long-latency neural feedback mechanisms to intervene, which may be preferential for movements requiring maneuverability versus stability. Local joint stiffness of muscles was determined by the stabilizing or destabilizing effects of moment-arm versus joint angle relationships. By preferentially activating muscles with high local stiffness, muscle activation patterns with feedforward stabilizing properties could be selected. Such a strategy may increase intrinsic postural stability without co-contraction, and may be useful criteria in the force-sharing problem.

Keywords: Neuromuscular; Biomechanical model; Posture; Balance; Cat hindlimb; Motor control; Modes of movement; Moment arm; Neuromechanics; Force sharing; Muscle activation pattern; Feedforward neural control

1. Introduction

Maintaining standing balance is an important motor function where the overall task is to stabilize the body center of mass (CoM) by generating the appropriate forces in each limb. However, each limb has multiple muscles acting at many joints—more degrees of freedom than the joint torques specified by the task—suggesting a wide range of muscular coordination strategies is possible (Bernstein, 1967), even within a single limb.

The stability of the limb configuration is part of the postural task that could resolve this neuromuscular redundancy. Muscle activity in response to a perturbation occurs after 50 ms in a cat, and electromechanical delays of the musculoskeletal system add another 50 ms delay before stabilizing forces are produced (Horak and Macpherson, 1996). A feedforward neural strategy of choosing an intrinsically stabilizing muscle activation pattern would potentially reduce the necessity for active neural feedback as well as decrease the number of candidate muscle activation patterns for performing the postural task.

Several mechanisms in the musculoskeletal system can provide instantaneous mechanical stability as a function of muscle activation patterns. The length–tension (Gordon et al., 1966; Rack and Westbury, 1974), and force–velocity

*Corresponding author at: The Wallace H. Coulter Department of Biomedical Engineering at Georgia Tech and Emory University, 313 Ferst Drive, Atlanta, GA 30322-0535, USA. Tel.: +1 40 489 45 216.
E-mail address: lena.ting@bme.gatech.edu (L.H. Ting).

0021-9290/$ - see front matter © 2008 Elsevier Ltd. All rights reserved.
doi:10.1016/j.jbiomech.2008.02.004

(Gasser and Hill, 1924) relationships of muscle are inherently stabilizing and depend monotonically on muscle activation; stronger activation results in greater viscoelasticity (Rack and Westbury, 1969). Muscle moment arms also change with joint motion, altering the net torque produced at a joint, and can contribute to either joint stability or instability (Young et al., 1992). Although these intrinsic musculoskeletal properties provide instantaneous feedback in response to perturbations, it has not been established whether they are sufficient to stabilize limb posture in a variety of animals and tasks (Edwards, 2007; Morasso and Sanguineti, 2002; Morasso and Schieppati, 1999; Richardson et al., 2005; Winter et al., 1998, 2001).

In this study, we hypothesized that the muscular redundancy in postural control is reduced when muscle activation patterns are chosen with respect to both intrinsic musculoskeletal stability and endpoint force production. We evaluated our hypothesis using Lyapunov stability theory applied to the linearized mathematical model of the feline hindlimb (Burkholder and Nichols, 2004) activated with a large set of muscle activation patterns that produced identical endpoint forces. We found that a reduced set of stabilizing muscle activation patterns exists, but that the relationship between individual muscle characteristics and whole-limb stability is not straightforward.

2. Methods

2.1. Methods overview

We used a computational model to analyze the relationship of whole-limb mechanical stability of the cat hindlimb to individual muscle properties. The model is three-dimensional, has physiologically relevant degrees of freedom, and experimentally determined muscle properties (Burkholder and Nichols, 2000, 2004; Roy et al., 1997; Sacks and Roy, 1982). We generated a set of muscle activation patterns that produced the identical postural endpoint force and examined the model response to small disturbances to the limb for each muscle activation pattern. Using linear system-analysis tools (Alexandrov et al., 2005; Szidarovszky and Bahill, 1992), we quantified the patterns of limb motion (limb modes) in response to disturbances, and the rate (eigenvalues) at which the whole-limb configuration returned to or moved away from the initial position. To determine individual muscle contributions to whole-limb stability we compared the local (joint-level) stiffness of muscles to the stability of the limb modes. Finally, we constructed muscle activation patterns based on the local stiffness of muscles and compared the whole-limb stability of these patterns to the randomly generated patterns.

2.2. Musculoskeletal model

The model had three degrees of freedom at the hip, and two each at the knee and ankle (Burkholder and Nichols, 2004; McKay et al., 2007; van Antwerp et al., 2007). The pelvis was fixed and the foot was connected to the ground through a pin joint at the metatarsophalangeal joint (MTP) leaving 4 degrees of freedom. The equations of motion for the model were expressed in the generalized coordinate system, $\theta = [\theta_{HF}, \theta_{HA}, \theta_{HR}, \theta_{KE}, \theta_{KA}, \theta_{AE}, \theta_{AA}]^T$, where the subscripts denote the positive direction of joint movement: hip flexion (HF), hip adduction (HA), hip external rotation (HR), knee extension (KE), knee adduction (KA), ankle extension (AE), and ankle adduction (AA). Limb motion was described by the equations of motion:

$$\ddot{\vec{\theta}} = \mathbf{M}^{-1}[-\vec{V}(\vec{\theta},\dot{\vec{\theta}}) - \vec{G}(\vec{\theta}) + \mathbf{R}(\vec{\theta})\mathbf{F}_{MAX}(\vec{\theta},\dot{\vec{\theta}})\,\vec{\varepsilon} - \mathbf{J}(\vec{\theta})^T\vec{F}_{MTP}(\vec{\theta},\dot{\vec{\theta}})], \quad (1)$$

where $\mathbf{M}$ is the inertia matrix, $\vec{V}$ is the vector of centrifugal and Coriolis torques, $\vec{G}$ is the vector of gravitational torques, $\mathbf{R}$ is the moment-arm matrix, $\mathbf{F}_{MAX}$ is a diagonal matrix whose components are the maximum individual muscle forces corrected for pennation angle, $\vec{\varepsilon}$ is the vector of muscle activation levels ($0 \leqslant \vec{\varepsilon} \leqslant 1$), $\mathbf{J}^T$ is the transpose Jacobian mapping of external force at the MTP to joint torques, F_{MTP} is the resultant force at the MTP which is calculated using the constraint that translational acceleration of the MTP be zero. Thirty-one muscles were modeled using an adaptation of the Hill muscle model (Zajac, 1989) using architectural parameters taken from the literature (Roy et al., 1997; Sacks and Roy, 1982). The stiffness of each muscle was set to 3 F_{MAX}/L_F^0, where F_{MAX} is the maximal force of the muscle and L_F^0 is optimal fiber length. This value is near maximal stiffness described by the length–tension curve (Gordon et al., 1966) and the analysis was repeated for varying levels of stiffness.

2.3. Selection of muscle activation patterns

Postural muscle activation patterns ($\vec{\varepsilon}$) were chosen to produce the endpoint force vector measured experimentally in standing cats, $\vec{F}_{MTP}^0$, when the model was placed in an initial posture matched to kinematic data (Torres-Oviedo et al., 2006):

$$\mathbf{R}\mathbf{F}_{MAX}\,\vec{\varepsilon} = \vec{G} + \mathbf{J}^T\vec{F}_{MTP}^0. \quad (2)$$

Eq. (2) is redundant and has a 24-dimensional solution space (null space). To span the $\vec{\varepsilon}$ solution space, activation sets were chosen by projecting a random activation vector, $0 \leqslant \vec{\varepsilon}_0 \leqslant 1$ into the solution space using the quadratic cost function

$$c = (\vec{\varepsilon} - \vec{\varepsilon}_0)^T(\vec{\varepsilon} - \vec{\varepsilon}_0) \quad (3)$$

and constraints,

$$\mathbf{R}\mathbf{F}_{MAX}(\vec{\varepsilon} - \vec{\varepsilon}_0) = \vec{G} + \mathbf{J}^T\vec{F}_{MTP}^0 - \mathbf{R}\mathbf{F}_{MAX}\,\vec{\varepsilon}_0, \quad (4)$$

$$\vec{0} - \vec{\varepsilon}_0 \leqslant (\vec{\varepsilon} - \vec{\varepsilon}_0) \leqslant \vec{1} - \vec{\varepsilon}_0. \quad (5)$$

The optimization yields an activation set $\vec{\varepsilon}$ which produces the desired endpoint force, has all muscle activations between 0 and 1, and minimizes the distance to $\vec{\varepsilon}_0$. The test population consisted of 10,000 activation sets, which was large enough for the mean and covariance of activation level of 23 of the 31 modeled muscles to converge (Valero-Cuevas et al., 2003). Five of eight nonconvergent muscles had knee-flexor moment arms, and thus were not expected to be highly active in standing. Increasing the sample size 12-fold resulted in convergence of only three additional muscles, and orders of magnitude more samples were required for the remaining muscles to converge.

2.4. Whole-limb stability of muscle activation patterns

To determine whether a given muscle activation pattern $\vec{\varepsilon}$ produced a stable limb configuration, Eq. (1) was linearized by Taylor-series expansion about the initial posture at rest, and Lyapunov stability theory was applied to resulting linear, time-invariant state matrix. If all of the eigenvalues of the state matrix are negative, then the system is asymptotically stable such the limb will always return to the equilibrium posture under small perturbations (Szidarovszky and Bahill, 1992). The derivation of the dynamic equations of motion including the muscle model equations, and the linearization were performed using custom Matlab (Mathworks, Inc., Natick, MA, USA) routines (www.neuromechanic.com).

For each muscle activation pattern, the eigenvectors of the state matrix (limb modes), represent coordinated movements of joints and define a

Please cite this article as: Bunderson, N.E., et al., Reduction of neuromuscular redundancy for postural force generation using an intrinsic stability criterion. Journal of Biomechanics (2008), doi:10.1016/j.jbiomech.2008.02.004

basis spanning all possible limb motion for the linearized system (Alexandrov et al., 2005). To compare across muscle activation patterns, the limb modes were grouped by hierarchical cluster analysis. Distance between eigenvectors was computed using the Euclidean distance between vectors and the cluster hierarchy was created using Ward's linkages (Ramsay and Silverman, 2005). The number of clusters was determined by the greatest average link height with inconsistent with lower linkages. In order to have a physically interpretable metric of stability, the real component of the eigenvalue was converted to the perturbation halving time:

$$t_{50} \equiv \frac{\ln(0.5)}{\mathrm{Re}(\lambda)}, \tag{6}$$

where λ is the eigenvalue corresponding to the limb mode. A restatement of the Lyapunov criteria for asymptotic stability is that a given muscle activation pattern $\vec{\varepsilon}$ produces a stable limb configuration if t_{50} for all limb modes is positive. Negative values of t_{50} ($\lambda > 0$) represent the perturbation doubling time in an unstable limb.

To determine whether a limb stability criterion could reduce the redundancy of muscle activation patterns, we compared the total muscle activation set to the subset of stable muscle activation patterns. We compared the range of activation for each muscle and the number of principal components required to account for 95% of the variability in each set.

2.5. Stability contribution of individual muscles

To determine whether specific muscles were associated with whole-limb stability, we calculated correlation coefficients between limb-mode eigenvalues and muscle activation levels. We used a threshold of $|r| > 0.4$ to determine substantial correlation for 31 degrees of freedom (all $p < 10^{-35}$).

We also determined whether individual muscle contributions to joint stiffnesses were predictive of whole-limb stability across the set of muscle activation patterns. Each muscle crosses more than one degree of freedom (e.g. knee flexion/extension and knee ab/adduction) and therefore contributes to multiple joint stiffnesses when activated. Because the stiffness of the muscle across the joints are not independent, we quantified the contributions of each muscle to the joint stiffness by computing the eigenvalues of the stiffness matrix for each muscle (e.g. the Jacobian of muscle torque with respect to all of the degrees of freedom crossed by that muscle). As a metric of stability, we defined the terms *maximum local positive stiffness* (κ_i^+), *maximum local negative stiffness* (κ_i^-), and *mean local* ($\bar{\kappa}_i$) *stiffness* for each muscle such that:

$$\kappa_i^+ = \max\left[\mathrm{eig}\left(\frac{\partial(\vec{R}_i F_{M,i})}{\partial\theta}\right) > 0\right],$$

$$\kappa_i^- = \min\left[\mathrm{eig}\left(\frac{\partial(\vec{R}_i F_{M,i})}{\partial\theta}\right) < 0\right],$$

$$\bar{\kappa}_i = \mathrm{mean}\left[\mathrm{eig}\left(\frac{\partial(\vec{R}_i F_{M,i})}{\partial\theta}\right)\right].$$

2.6. Prediction of stable muscle activation patterns

To determine whether local muscle stiffness could be used to restrict the set of muscle activation patterns for standing posture, we replaced the cost function (5), with one weighted by each muscle's mean local stiffness ($\bar{\kappa}_i$):

$$c = (1-\mu)(\vec{\varepsilon} - \vec{\varepsilon}_0)^{\mathrm{T}}(\vec{\varepsilon} - \vec{\varepsilon}_0) - \mu\vec{\bar{\kappa}}_i^{\mathrm{T}}(\vec{\varepsilon} - \vec{\varepsilon}_0). \tag{7}$$

We then evaluated whole-limb stability of muscle activation patterns generated as a function of μ. A value of $\mu = 1$ resulted in a single unique activation set regardless of the random activation guess $\vec{\varepsilon}_0$.

Finally, to verify the robustness of results to a weight-bearing configuration, the entire analyses were recomputed with the fixed pelvis constraint relaxed to allow a single translational degree of freedom in the vertical direction. To satisfy equilibrium, the weight of the pelvis was set to a value of about 1/4 the weight of a cat, such that the combined weight of the pelvis and limb was equal to the vertical component of the ground reaction force.

3. Results

3.1. Mechanical modes

Whole-limb motion was characterized by four limb-mode clusters (graphical representations in Fig. 1). The first mode

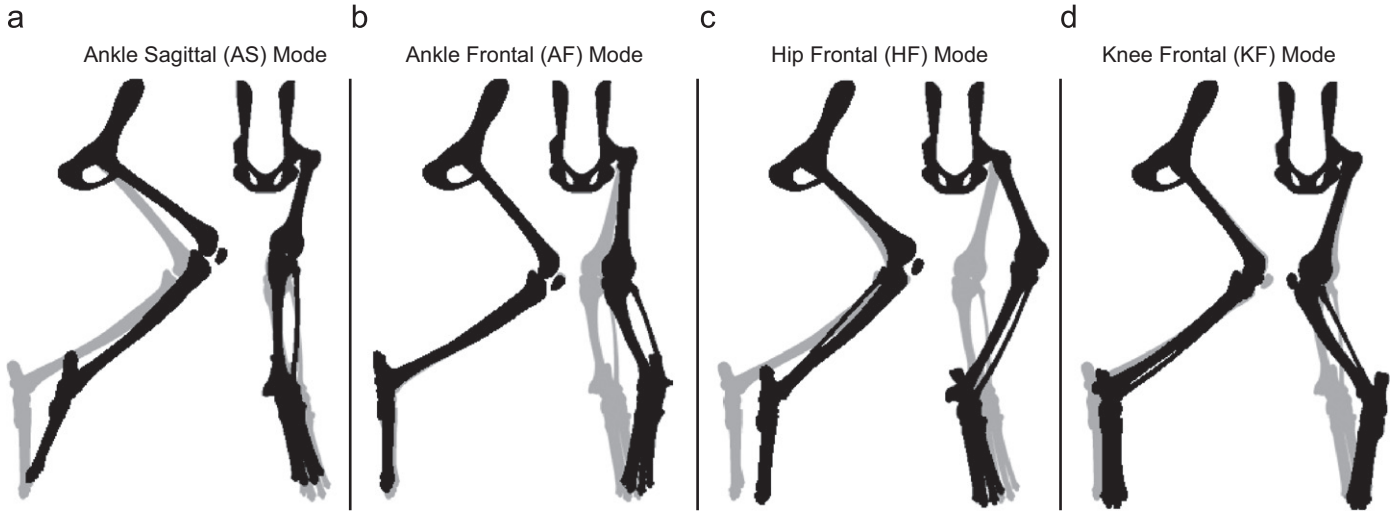

Fig. 1. Mechanical modes of the limb. Four limb modes characterized the whole-limb motion following perturbations: (A) the ankle sagittal (AS) mode is dominated by flexion and extension of the ankle, but includes motion at all joints. (B–D) The remaining three modes are dominated by motions in the frontal plane. The gray limb represents the nominal limb posture. The black limb represents the limb displacement associated with each of the four modes describing limb motion. Note that this appears to displace the toe from its endpoint constraint in some cases because the eigenvectors are scaled for illustrative purposes. The modes are a feature of the linearized model and are valid only for small angle displacements.

Please cite this article as: Bunderson, N.E., et al., Reduction of neuromuscular redundancy for postural force generation using an intrinsic stability criterion. Journal of Biomechanics (2008), doi:10.1016/j.jbiomech.2008.02.004

can be approximately described as ankle motion in the sagittal-plane (AS) (Fig. 1A). The remaining three modes can be described primarily as frontal-plane motion of the ankle (AF), hip (HF), and knee (KF) (Fig. 1B–D). Limb modes with t_{50} faster than 7 ms were not examined, as they were all unconditionally stable, and faster than physiological timescales relevant to postural control. The included angle between the means of the four clusters ranged from a maximum of 102° between AS and AF to a minimum of 69° between AS and HF with an average inter-cluster distance of 88° and an average intra-cluster distance of 13°.

3.2. Stability of all muscle activation patterns

Only 35% of the muscle activation patterns were stable in all limb modes (Table 1). Two modes (KF and HF, Fig. 2) were stable for greater than 99.5% of muscle activation patterns (Table 1). The remaining two were stable for 88% (AF) and 37% (AS) of activation patterns,

Table 1
Stability characterization of each limb mode

	AS	AF	HF	KF	ALL
% Stable	37	88	99.5	100	35
t_{50} (s) stable modes	0.224–68	0.125–60	0.228–45	0.007–0.036	
t_{50} (s) unstable modes	0.062–67	0.065–67	0.088–35		
Mean t_{50} (s) stable	0.683	0.270	0.387	0.020	
Mean t_{50} (s) unstable	−0.305	−0.436	−0.359		

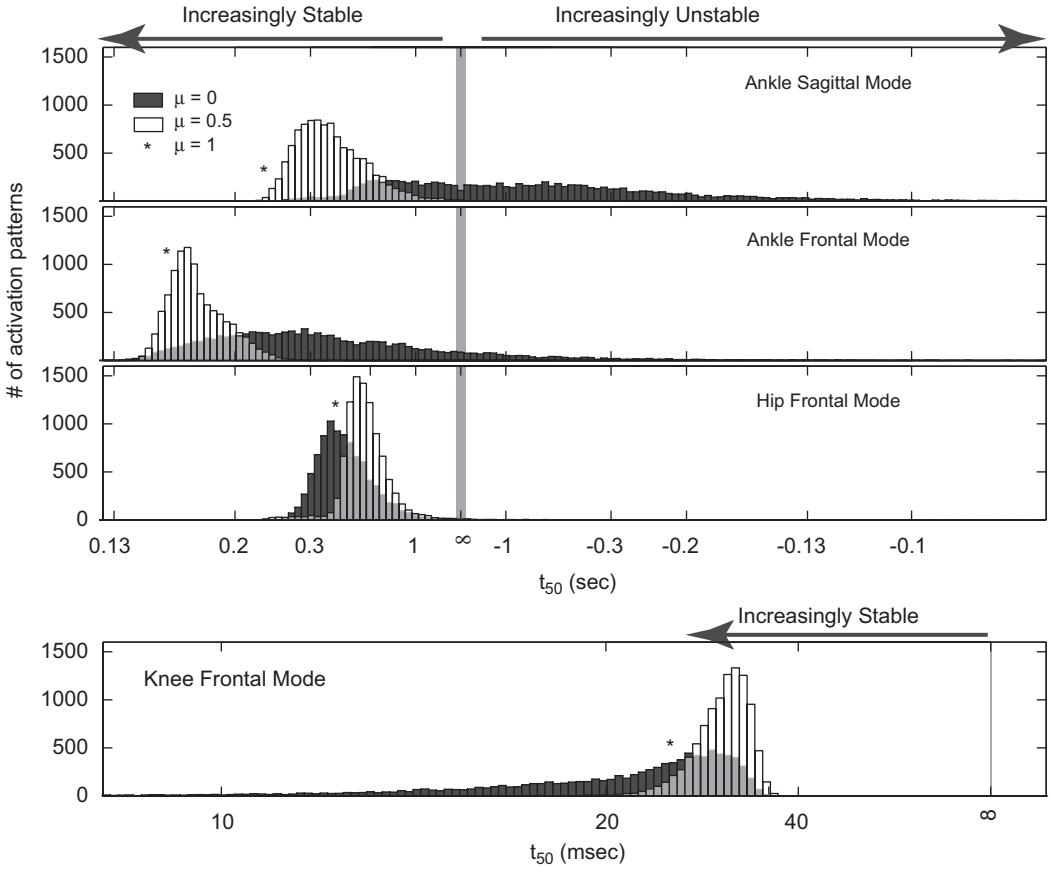

Fig. 2. Histogram of limb stability for each mode across all muscle activation patterns. Histograms show the number of activation sets for each binned eigenvalue range for each limb mode. Limb modes with positive finite t_{50} (eigenvalues less than 0) are stable and limb modes with negative finite t_{50} (eigenvalues greater than 0) are unstable. The gray band centered at neutral stability ($t_{50} = \infty$) spans all limb modes with doubling-time magnitude greater than 10 s. The dark gray histogram shows the distribution of stability of each mode for the set of random activation patterns ($\mu = 0$), for which (A) the AS mode was stable for 37% of muscle activation patterns, (B) the AF mode was stable for 88%, (C) the HF was stable for 99.5%, and (D) the KF mode was stable for 100% of muscle activation patterns. The white histogram shows the distribution of the stability of the limb when the selection of muscle activation patterns was biased toward locally stiff muscles ($\mu = 0.5$). The asterisk represents the t_{50} value for the unique muscle activation pattern that maximized the activation of locally stiff muscles ($\mu = 1$). 35% of the patterns resulted in a limb with negative eigenvalues (stable) in all modes.

Please cite this article as: Bunderson, N.E., et al., Reduction of neuromuscular redundancy for postural force generation using an intrinsic stability criterion. Journal of Biomechanics (2008), doi:10.1016/j.jbiomech.2008.02.004

respectively (Fig. 2 and Table 1). KF was the fastest mode with $|t_{50}|$ between 7 and 36 ms, while all other modes were slower than 62 ms (Table 1).

3.3. Stability contribution of individual muscles

The range of activation levels within each muscle were similar in the stable and unstable sets, with only a 4% average decrease in the range of muscle activation levels between the two sets; only Gluteus Medius (GMED) decreased in range of activation by more than 10%. Fifteen principal components were required to account for 95% of the variability in both stable and total sets.

Few correlations were found between individual muscle activation levels and limb-mode stability (Fig. 3a). HF and KF stability were most strongly correlated with inactivation of Biceps Femoris, posterior compartment (BFP) and Rectus Femoris (RF) ($r = 0.52$ and 0.57, respectively, for HF; $r = 0.83$ and $r = 0.72$, respectively, for KF) (Fig. 3a, 3rd and 4th column, asterisks). AF stability was most strongly correlated with activation of Tibialis Posterior (TP) and Peroneus Brevis (PB) ($r = -0.45$, and -0.68, respectively), and deactivation of Flexor Hallucis Longus (FHL, $r = 0.51$) (Fig. 3a, 1st column, asterisks). AS stability was most strongly correlated with activation of Medial Gastrocnemius (MG, $r = -0.78$), VL ($r = -0.52$), and EDL ($r = -0.40$), and deactivation of FHL ($r = 0.60$) (Fig. 3a, 2nd column, asterisks).

No consistent relationships between local stiffness of activated muscles and whole-limb stability were found (Fig. 3a and b). Most muscles had stronger positive than negative local stiffness (i.e. the magnitude of κ_i^+ (Fig. 3a, black bars) was greater than the magnitude of κ_i^- (Fig. 3b, white bars)). In AS, stability was strongly correlated with MG, VL, and EDL activation, but only MG had greater than average local positive stiffness (Fig. 3b).

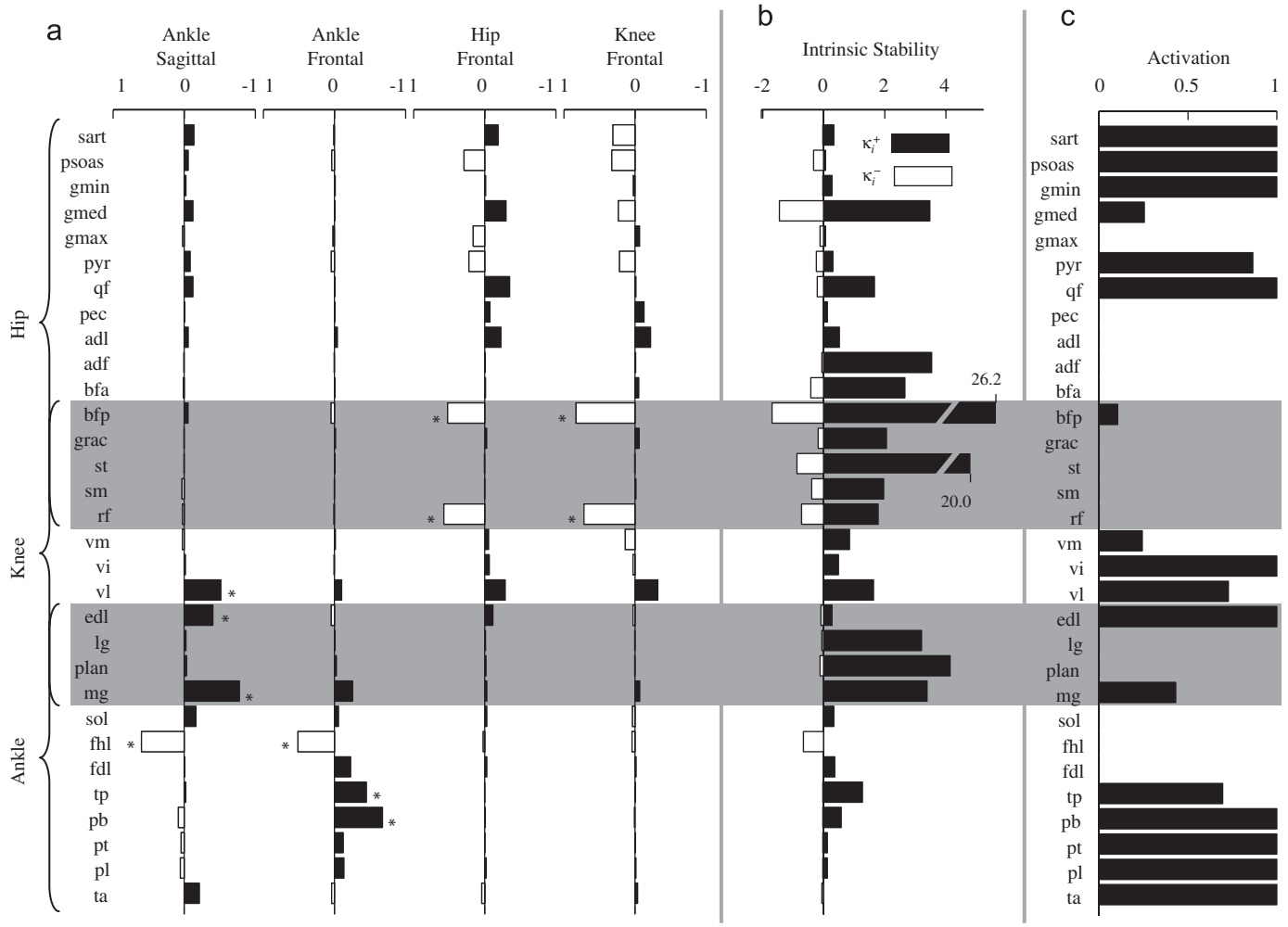

Fig. 3. Relationship between overall limb stability, individual muscle activation levels, and joint-level stiffness of individual muscles. Gray bars indicate biarticular muscles: (A) correlation coefficients of individual muscle activation with eigenvalues of each mode. Negative correlation coefficients indicate that activation of the muscle correlates with increased modal stability (decreased eigenvalue). Muscles with statistically significant correlation coefficient magnitudes of greater than 0.4 are indicated by an asterisk (*). In general, hip and knee muscles are correlated with HF and KF stability and knee and ankle muscles are correlated with AS and AF stability. (B) The maximum local positive (black bars, κ_i^+) and negative (white bars, κ_i^-) stiffness for each muscle. (C) The muscle activation pattern generated when using a cost function maximizing activation of muscles with high local stiffness ($\mu = 1$, Eq. (7)) results in a unique activation pattern with strong coactivation of hip and ankle uniarticular muscles.

Please cite this article as: Bunderson, N.E., et al., Reduction of neuromuscular redundancy for postural force generation using an intrinsic stability criterion. Journal of Biomechanics (2008), doi:10.1016/j.jbiomech.2008.02.004

The activation of these four muscles was highly correlated because they are mutually advantageous when standing up against gravity (data not shown). KF stability was negatively correlated with activation of BFP, the muscle with the greatest positive local stiffness. Although BFP had the large maximum local stiffness, it also had substantial negative local stiffness values as well, highlighting the difficulty of assigning responsibility of whole-limb stability to the characteristics of a particular muscle.

3.4. Prediction of a stable set of muscle activation patterns

An increasingly stable set of muscle activation patterns was found when muscles with large mean local stiffness were preferentially selected (i.e. weighting factor μ, Eq. (7), was increased) (Fig. 4a). For $\mu > 0.5$, all muscle activation patterns were stable in all modes (Figs. 2 and 4). The number of principal components decreased monotonically with μ (Fig. 4a); a value of $\mu = 1$ resulted in a unique activation pattern (Fig. 3c). This activation pattern was in the 99.96th percentile of stability in mode AS, and the 96, 59, and 42 percentile of stability in modes AF, HF, and KF, respectively (Fig. 2, asterisks).

In contrast, as intrinsic stiffness of individual muscles was increased from the nominal value of $3F_{MAX}/L_F^0$, the number of stable muscle activation patterns increased monotonically, but the number of principal components to describe 95% of data variability remained at 15 (Fig. 4b). At stiffness values of $0.3F_{MAX}/L_F^0$, corresponding to the stiffness of the length–tension curve at 95% optimal fiber length, no stable muscle activation patterns were found. To generate a set with 97% stable muscle activation patterns, intrinsic stiffness had to be increased to 8, which cannot be achieved from the length–tension property of muscle alone, but is less than the short-range stiffness of muscle (Rack and Westbury, 1974).

Allowing the pelvis to move vertically did not substantially change the results. In addition to AS, AF, HF, and KF modes, a fifth mode, comprised mostly of hip and knee flexion/extension, was created that was stable for 99% of the activation patterns. The proportion of total stable muscle activation patterns decreased by 4%, and the correlation of local muscle stability to whole-limb stability was unaffected.

4. Discussion

Within the large set of activation patterns that satisfy the force requirement for posture, a reduced subset of the same dimensional complexity produced mechanical limb stability, and few strong correlations between specific muscles and stability were found. This suggests that the stability criterion restricts the size of the muscle activation solution space without restricting the muscle activation strategy.

Based on intrinsic musculoskeletal properties, muscle activation patterns may be chosen by the nervous system to set the relative mechanical stability or maneuverability of the limb in addition to meeting the kinetic constraints of a task. It has been suggested that muscles operate near optimum length, where muscle stiffness due to the length–tension relationship is close to zero. There were no globally stable muscle activation patterns for muscle stiffnesses in this range (<1), although the KF and HF modes were stable. In contrast, essentially no unstable activation patterns were found for muscle stiffnesses greater than 8. At its maximum slope, the length–tension relationship has a stiffness of 4, which may be increased as much as four-fold by the autogenic stretch reflex (Nichols and Houk, 1976), suggesting, along with short-range stiffness contributions (Epstein and Herzog, 2003), that these mechanisms alone may be adequate to ensure limb stability. Supporting this idea, cats with spinal cord transection are able to stand independently and resist small perturbations (De Leon et al., 1998; Pratt et al., 1994), but do not generate direction-specific postural responses (Macpherson and Fung, 1999). Our model demonstrated that even when the limb is unstable, the

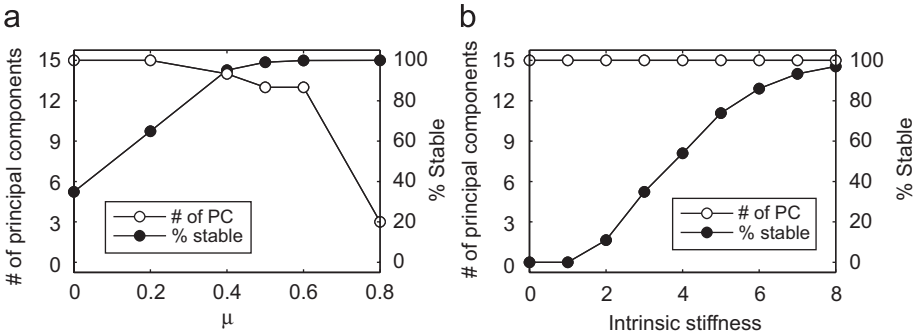

Fig. 4. Changes in activation set dimensionality and stability due to biasing of the activation sets to locally stiff muscles and to varying magnitudes of intrinsic muscle stiffness. Randomized set of muscle activity were generated for different values of μ, weighting the cost function in favor of locally stabilizing muscles, and at different stiffness values for the muscles: (A) as the weighting toward locally stable muscle increases, the percentage of stable muscle activation patterns within each randomized set increases, and the number of principal components accounting for 95% variability of the set decreases. (B) As intrinsic stiffness (normalized to the maximum force generating capability of the muscle times the optimal fiber length) increases, the percentage of stable muscle activation patterns increases without decreasing the number of principal components describing 95% variability of the set.

Please cite this article as: Bunderson, N.E., et al., Reduction of neuromuscular redundancy for postural force generation using an intrinsic stability criterion. Journal of Biomechanics (2008), doi:10.1016/j.jbiomech.2008.02.004

perturbation doubling-time was greater than 100 ms, approximately the latency of active force-generation in postural responses (50 ms muscle activation latency plus 50 ms electromechanical delay) (Macpherson, 1988). The viscous force–velocity relationship of muscle contributes significantly to prolonging the perturbation doubling-time, illustrating its importance to postural control.

Neural control may be dedicated more towards sagittal-plane control and ankle control, consistent with the primary joint motions of the limb in both locomotion and posture. The high stability of non-sagittal modes in our analysis suggests that frontal-plane control of these joints does not require substantial neural control and reflects inherently stabilizing non-sagittal moment arms (Young et al., 1992). The relative instability of ankle flexion/extension and ad/abduction modes is consistent with the important role of the ankle in directing the actions of more proximal muscles (Fregly and Zajac, 1996; Ting et al., 1999; van Antwerp et al., 2007; Zajac, 2002), which may be particularly important during perturbations (Daley et al., 2007).

Our analysis highlights two strategies by which postural stability from musculoskeletal properties may be increased. For novel environments, it may be advantageous to increase limb stability through co-contraction (Osu et al., 2002). In contrast, biasing selection of muscle activation patterns to locally stiff muscles, due to moment-arm properties can also result in whole-limb stability without need for co-contraction. These two different strategies may explain our prior data demonstrating different muscle activation patterns across individuals during quiet standing (Torres-Oviedo et al., 2006; Torres-Oviedo and Ting, 2007). Similarly, some subjects maintain trunk rotational stiffness through feedforward activation of muscles, whereas others modulate muscle activation in response to trunk motion (Gurfinkel et al., 2006). Our results demonstrate the vast number of possible muscle activation patterns that could stabilize the limb. We propose that individual variations in the selection of a muscle activation pattern may result from differential tradeoffs between stability, energetic efficiency, and other factors (Ting and McKay, 2008; Lockhart and Ting, 2007; Welch and Ting, 2008).

It may be possible to increase stability of musculoskeletal simulations for a range of dynamics tasks by considering muscle stiffness and moment-arm properties in optimizations of muscle activation patterns. While activation of locally stabilizing muscles did not guarantee whole-limb stability in our analysis, it was possible to increase probability of whole-limb stability preferentially selecting muscles with greater local joint stiffness. Our approach may be extendible to more dynamic simulations of locomotion (Higginson et al., 2006; Neptune et al., 2001), and be used to choose muscle activation patterns that increase the stability of the simulations, helping to maintain the body on a particular cyclic trajectory (Holmes et al., 2006).

Conflict of interest

We have no conflict of interest to report.

Acknowledgements

Supported by NIH Grants HD46922 and HD032571. The NIH had no role in the design, performance, or interpretation of the study.

References

Alexandrov, A.V., Frolov, A.A., Horak, F.B., Carlson-Kuhta, P., Park, S., 2005. Feedback equilibrium control during human standing. Biological Cybernetics 1–14.

Bernstein, N., 1967. The Coordination and Regulation of Movements. Pergamon Press, New York.

Burkholder, T.J., Nichols, T.R., 2000. The mechanical action of proprioceptive length feedback in a model of cat hindlimb. Motor Control 4, 201–220.

Burkholder, T.J., Nichols, T.R., 2004. Three-dimensional model of the feline hindlimb. Journal of Morphology 261, 118–129.

Daley, M.A., Felix, G., Biewener, A.A., 2007. Running stability is enhanced by a proximo-distal gradient in joint neuromechanical control. Journal of Experimental Biology 210, 383–394.

De Leon, R.D., Hodgson, J.A., Roy, R.R., Edgerton, V.R., 1998. Full weight-bearing hindlimb standing following stand training in the adult spinal cat. Journal of Neurophysiology 80, 83–91.

Edwards, W.T., 2007. Effect of joint stiffness on standing stability. Gait & Posture 25, 432–439.

Epstein, M., Herzog, W., 2003. Aspects of skeletal muscle modelling. Philosophical Transactions of the Royal Society of London Series B: Biological Sciences 358, 1445–1452.

Fregly, B.J., Zajac, F.E., 1996. A state-space analysis of mechanical energy generation, absorption, and transfer during pedaling. Journal of Biomechanics 29, 81–90.

Gasser, H.S., Hill, A.V., 1924. The dynamics of muscular contraction. Proceedings of the Royal Society of London Series B: Biological Sciences 96, 398–437.

Gordon, A.M., Huxley, A.F., Julian, F.J., 1966. The variation in isometric tension with sarcomere length in vertebrate muscle fibres. Journal of Physiology 184, 170–192.

Gurfinkel, V., Cacciatore, T.W., Cordo, P., Horak, F., Nutt, J., Skoss, R., 2006. Postural muscle tone in the body axis of healthy humans. Journal of Neurophysiology 96, 2678–2687.

Higginson, J.S., Zajac, F.E., Neptune, R.R., Kautz, S.A., Delp, S.L., 2006. Muscle contributions to support during gait in an individual with post-stroke hemiparesis. Journal of Biomechanics 39, 1769–1777.

Holmes, P., Full, R., Koditschek, D.E., Guckenheimer, J., 2006. The dynamics of legged locomotion: models, analyses, and challenges. SIAM Review 48, 207–304.

Horak, F.B., Macpherson, J.M., 1996. Postural orientation and equilibrium. In: Rowell, L.B., Shepherd, J.T. (Eds.), Handbook of Physiology, Section 12. American Physiological Society, New York, pp. 255–292.

Lockhart, D.B., Ting, L.H., 2007. Optimal feedback transformations for balance. Nature Neuroscience 10, 1329–1336.

Macpherson, J.M., 1988. Strategies that simplify the control of quadrupedal stance. II. Electromyographic activity. Journal of Neurophysiology 60, 218–231.

Macpherson, J.M., Fung, J., 1999. Weight support and balance during perturbed stance in the chronic spinal cat. Journal of Neurophysiology 82, 3066–3081.

McKay, J.L., Burkholder, T.J., Ting, L.H., 2007. Biomechanical capabilities influence postural control strategies in the cat hindlimb. Journal of Biomechanics 40, 2254–2260.

Please cite this article as: Bunderson, N.E., et al., Reduction of neuromuscular redundancy for postural force generation using an intrinsic stability criterion. Journal of Biomechanics (2008), doi:10.1016/j.jbiomech.2008.02.004

Morasso, P.G., Schieppati, M., 1999. Can muscle stiffness alone stabilize upright standing? Journal of Neurophysiology 82, 1622–1626.

Morasso, P.G., Sanguineti, V., 2002. Ankle muscle stiffness alone cannot stabilize balance during quiet standing. Journal of Neurophysiology 88, 2157–2162.

Neptune, R.R., Kautz, S.A., Zajac, F.E., 2001. Contributions of the individual ankle plantar flexors to support, forward progression and swing initiation during walking. Journal of Biomechanics 34, 1387–1398.

Nichols, T.R., Houk, J.C., 1976. Improvement in linearity and regulation of stiffness that results from actions of stretch reflex. Journal of Neurophysiology 39, 119–142.

Osu, R., Franklin, D.W., Kato, H., Gomi, H., Domen, K., Yoshioka, T., Kawato, M., 2002. Short- and long-term changes in joint co-contraction associated with motor learning as revealed from surface EMG. Journal of Neurophysiology 88, 991–1004.

Pratt, C.A., Fung, J., Macpherson, J.M., 1994. Stance control in the chronic spinal cat. Journal of Neurophysiology 71, 1981–1985.

Rack, P.M., Westbury, D.R., 1969. The effects of length and stimulus rate on tension in the isometric cat soleus muscle. Journal of Physiology 204, 443–460.

Rack, P.M., Westbury, D.R., 1974. The short range stiffness of active mammalian muscle and its effect on mechanical properties. Journal of Physiology 240, 331–350.

Ramsay, J.O., Silverman, B.W., 2005. Functional Data Analysis. Springer, New York, Berlin.

Richardson, A.G., Slotine, J.J., Bizzi, E., Tresch, M.C., 2005. Intrinsic musculoskeletal properties stabilize wiping movements in the spinalized frog. Journal of Neuroscience 25, 3181–3191.

Roy, R.R., Kim, J.A., Monti, R.J., Zhong, H., Edgerton, V.R., 1997. Architectural and histochemical properties of cat hip 'cuff' muscles. Acta Anatomica (Basel) 159, 136–146.

Sacks, R.D., Roy, R.R., 1982. Architecture of the hind limb muscles of cats: functional significance. Journal of Morphology 173, 185–195.

Szidarovszky, F., Bahill, T., 1992. Linear Systems Theory. CRC Press, Boca Raton, FL.

Ting, L.H., McKay, J.L., 2008. Neuromechanics of muscle synergies for posture and movement. Current Opinion in Neurobiology in press, doi:10.1016/j.conb.2008.01.002.

Ting, L.H., Kautz, S.A., Brown, D.A., Zajac, F.E., 1999. Phase reversal of biomechanical functions and muscle activity in backward pedaling. Journal of Neurophysiology 81, 544–551.

Torres-Oviedo, G., Ting, L.H., 2007. Muscle synergies characterizing human postural responses. Journal of Neurophysiology 98, 2144–2156.

Torres-Oviedo, G., Macpherson, J.M., Ting, L.H., 2006. Muscle synergy organization is robust across a variety of postural perturbations. Journal of Neurophysiology 96, 1530–1546.

Valero-Cuevas, F.J., Johanson, M.E., Towles, J.D., 2003. Towards a realistic biomechanical model of the thumb: the choice of kinematic description may be more critical than the solution method or the variability/uncertainty of musculoskeletal parameters. Journal of Biomechanics 36, 1019–1030.

van Antwerp, K.W., Burkholder, T.J., Ting, L.H., 2007. Inter-joint coupling effects on muscle contributions to endpoint force and acceleration in a musculoskeletal model of the cat hindlimb. Journal of Biomechanics 40 (16), 3570–3579.

Welch, T.D., Ting, L.H., 2008. A feedback model predicts muscle activity during human postural responses to support surface translations. Journal of Neurophysiology 99, 1032–1038.

Winter, D.A., Patla, A.E., Prince, F., Ishac, M., Gielo-Perczak, K., 1998. Stiffness control of balance in quiet standing. Journal of Neurophysiology 80, 1211–1221.

Winter, D.A., Patla, A.E., Rietdyk, S., Ishac, M.G., 2001. Ankle muscle stiffness in the control of balance during quiet standing. Journal of Neurophysiology 85, 2630–2633.

Young, R.P., Scott, S.H., Loeb, G.E., 1992. An intrinsic mechanism to stabilize posture—joint-angle-dependent moment arms of the feline ankle muscles. Neuroscience Letters 145, 137–140.

Zajac, F.E., 1989. Muscle and tendon: properties, models, scaling, and application to biomechanics and motor control. Critical Reviews in Biomedical Engineering 17, 359–411.

Zajac, F.E., 2002. Understanding muscle coordination of the human leg with dynamical simulations. Journal of Biomechanics 35, 1011–1018.

Please cite this article as: Bunderson, N.E., et al., Reduction of neuromuscular redundancy for postural force generation using an intrinsic stability criterion. Journal of Biomechanics (2008), doi:10.1016/j.jbiomech.2008.02.004